# Supporting Information

## Impact of inner hydrophobicity of dendrimer nanomicelles on biodistribution: a PET imaging study

Tom Roussel[1%], Twiany Dubois[2,3%], Beatrice Louis[2,3], Erik Laurini[4], Ling Ding[1], Laure Balasse[3], Vincent Nail[2,3], Françoise Dignat-George[2], Suzanne Giorgio[1], Sabrina Pricl[4,5], Benjamin Guillet[2,3], Philippe Garrigue[2,3], Ling Peng[1,*]

[1] Aix Marseille University, CNRS, Centre Interdisciplinaire de Nanoscience de Marseille (CINaM), UMR 7325, Equipe Labellisée Ligue Contre le Cancer, Marseille, France

[2] Aix Marseille University, INSERM, INRAE, C2VN, Marseille, France

[3] Aix Marseille University, CNRS, CERIMED, Marseille, France

[4] Molecular Biology and Nanotechnology Laboratory, Department of Engineering and Architectures, University of Trieste, Trieste 34127, Italy

[5] Department of General Biophysics, Faculty of Biology and Environmental Protection, University of Lodz, Lodz 90-136, Poland

[%] These authors contributed equally to the study.

***Corresponding author:**

Dr Ling Peng

Aix Marseille Univ, CNRS, Centre Interdisciplinaire de Nanoscience de Marseille (CINaM), Marseille, France

Email: ling.peng@univ-amu.fr

ORCID: 0000-0003-3990-5248

## Table of content

**Table S1 PET/CT biodistribution quantifications** ..... 3

**Table S2 Gamma-counting biodistribution quantifications** ..... 4

**Table S3 Blood sampling quantifications** ..... 5

**Figure S1 Chemical characterization of AD-NOTA** ..... 6

**Figure S2 High-resolution mass spectrum of the dendrimer 4** ..... 7

**Figure S3 Surface zeta-potential of 4@ and 3@** ..... 8

**Figure S4 Computer simulations of 3@ and 4@** ..... 9

**Materials and methods** ..... 10

**Nuclear Magnetic Resonance** ..... 10

**Mass Spectrometry** ..... 10

**Synthesis and characterization of the amphiphilic dendrimer 3** ..... 11

**Synthesis and characterization of AD-3** ..... 11

**Synthesis and characterization of AD-4** ..... 12

**Synthesis and characterization of the amphiphilic dendrimer AD-NOTA** ..... 12

**Synthesis and characterization of the amphiphilic dendrimer 4** ..... 13

**Dynamic light scattering (DLS)** ..... 13

**Transmission Electron Microscopy (TEM)** ..... 14

**Critical micelle concentration (CMC)** ..... 14

**Isothermal titration calorimetry (ITC)** ..... 14

**Radiolabeling of [$^{68}$Ga]-4 and [$^{68}$Ga]-3** ..... 16

**Radiolabeling stability of [$^{68}$Ga]-4** ..... 16

**Animals** ..... 17

**PET/CT and gamma-counting biodistribution** ..... 17

**Statistics** ..... 18

**Computer simulations of 3@ and 4@** ..... 9

**Reference** ..... 18

**Table S1 PET/CT biodistribution quantifications**: 2h after injection of **[$^{68}$Ga]Ga-4@** and **[$^{68}$Ga]Ga-3@** in healthy mice and statistical analysis.

| Tissue | [$^{68}$Ga]Ga-4@ | | | [$^{68}$Ga]Ga-3@ | | | Post-hoc test *P* value |
|---|---|---|---|---|---|---|---|
| | %ID/cm$^3$ of tissue | | | | | | |
| | mean | sd | n | mean | sd | n | |
| **Liver** | 18 | 1.1 | 4 | 4.3 | 0.9 | 4 | <0.0001 |
| **Heart** | 9.4 | 2.2 | 4 | 7.1 | 1.6 | 4 | 0.8589 |
| Kidneys | 2.5 | 0.2 | 4 | 4.0 | 0.8 | 4 | 0.0204 |
| Lungs | 3.3 | 0.9 | 4 | 3.2 | 0.6 | 4 | >0.9999 |
| Brain | 1.2 | 0.3 | 4 | 0.5 | 0.1 | 4 | 0.0573 |
| Bone | 1.5 | 0.1 | 4 | 1.2 | 0.2 | 4 | 0.2315 |
| **Muscle** | 0.4 | 0.1 | 4 | 1.3 | 0.1 | 4 | <0.0001 |
| **Bladder** | 2.1 | 0.3 | 4 | 5.7 | 2.0 | 4 | 0.0017 |

**Table S2 Gamma-counting biodistribution quantifications**: 2h after injection of **[$^{68}$Ga]Ga-4@** and **[$^{68}$Ga]Ga-3**@ in healthy mice and statistical analysis.

| Tissue | [$^{68}$Ga]Ga-4@ | | | [$^{68}$Ga]Ga-3@ | | | Post-hoc test *P* value |
|---|---|---|---|---|---|---|---|
| | %ID/g of tissue | | | | | | |
| | mean | sd | n | mean | sd | n | |
| Liver | 9.8 | 1.9 | 4 | 4.5 | 0.7 | 4 | <0.0001 |
| Heart | 0.9 | 0.1 | 4 | 4.6 | 1.2 | 4 | <0.0001 |
| Kidneys | 1.5 | 0.2 | 4 | 7.6 | 1.5 | 4 | <0.0001 |
| Lungs | 1.4 | 0.2 | 4 | 6.3 | 0.9 | 4 | <0.0001 |
| Spleen | 2.7 | 0.3 | 4 | 3.4 | 0.6 | 4 | 0.9048 |
| Pancreas | 0.2 | 0.0 | 4 | 1.4 | 0.3 | 4 | 0.2313 |
| Brain | 0.1 | 0.0 | 4 | 0.4 | 0.1 | 4 | 0.9997 |
| Bone | 0.5 | 0.2 | 4 | 0.5 | 0.2 | 4 | >0.9999 |
| Muscle | 0.1 | 0.0 | 4 | 0.9 | 0.3 | 4 | 0.6894 |
| ANOVA *P* value | <0.0001 | | | | | | |

**Table S3 Blood sampling quantifications**: after injection of **[$^{68}$Ga]Ga-4@** and **[$^{68}$Ga]Ga-3@** in healthy mice and statistical analysis.

| **Time post injection** (min) | **[$^{68}$Ga]Ga-4@** | | | **[$^{68}$Ga]Ga-3@** | | | **Post-hoc test *P* value** |
|---|---|---|---|---|---|---|---|
| | %ID | | | | | | |
| | mean | sd | n | mean | sd | n | |
| 5 | 87.0 | 13.0 | 4 | 81.0 | 15.0 | 4 | 0.9750 |
| 15 | 83.0 | 14.0 | 4 | 69.0 | 16.0 | 4 | 0.4300 |
| 30 | 79.0 | 13.0 | 4 | 60.0 | 12.0 | 4 | 0.1321 |
| 45 | 73.0 | 10.0 | 4 | 57.0 | 11.0 | 4 | 0.2818 |
| 90 | 66.5 | 5.0 | 4 | 53.0 | 9.0 | 4 | 0.4721 |
| 120 | 57.0 | 3.0 | 4 | 48.0 | 7.0 | 4 | 0.8477 |
| ANOVA *P* value | 0.0004 | | | | | | |
| Non-linear regression $R^2$ | 0.5452 | | | 0.5152 | | | |
| Calculated half-life (fast, min) | 1.895 | | | 5.364 | | | |
| Calculated half-life (slow, min) | 577.8 | | | 247.0 | | | |

**Figure S1 Chemical characterization of AD-NOTA:** (**A**) $^{1}$H- and (**B**) $^{13}$C-NMR spectra of **AD-NOTA** recorded in $CDCl_3$/MeOD at 300K. (**C**) High-resolution mass spectrum in negative electrospray mode of [**AD-NOTA-**3H]$^{3-}$.

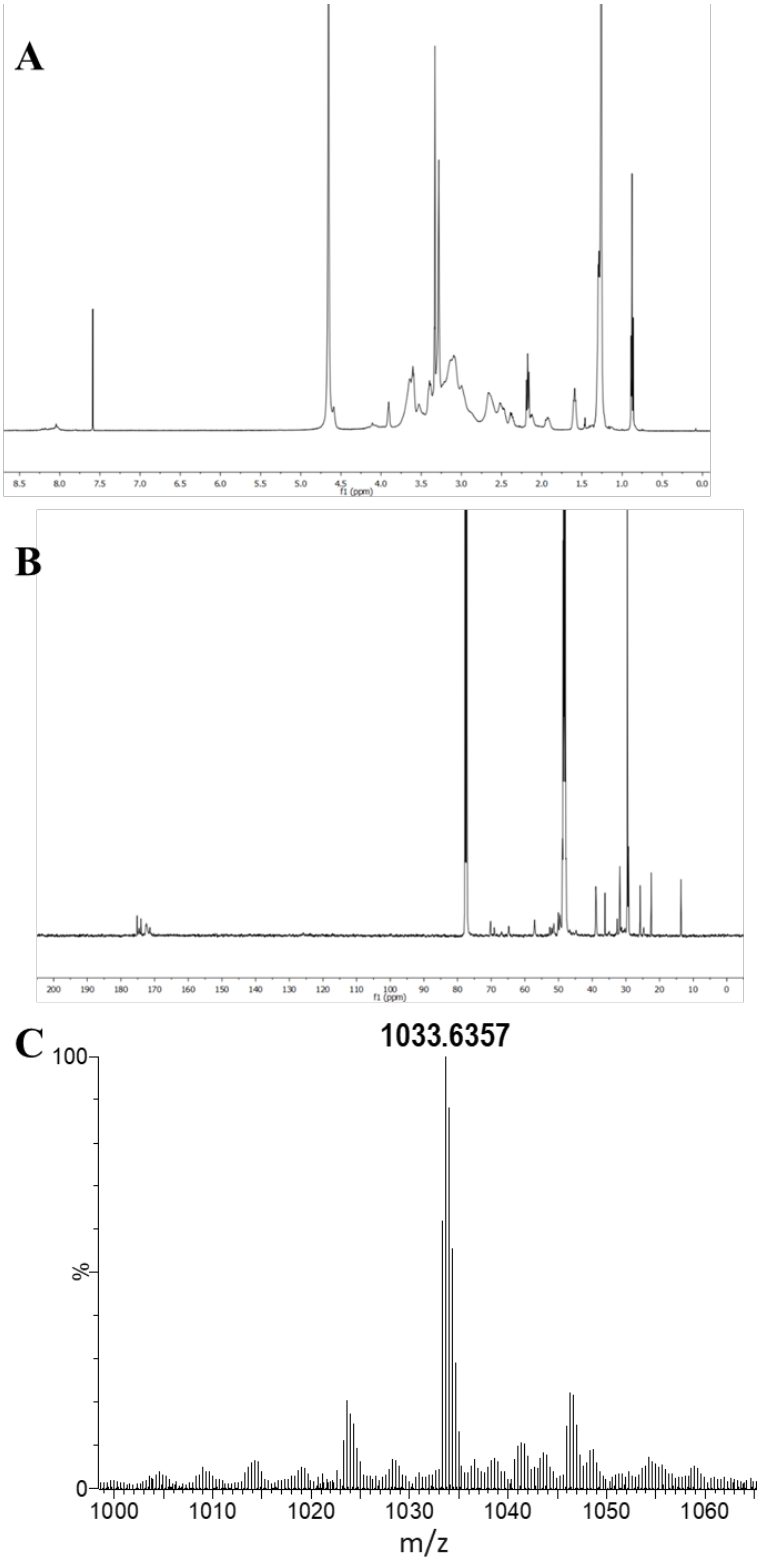

**Figure S2 High-resolution mass spectrum of the dendrimer 4:** High-resolution mass spectrum of the dendrimer **4** showing the isotopic pattern characteristic of the quadruple charged species [**4**+4H]$^{4+}$. The inset shows the calculated isotopic pattern.

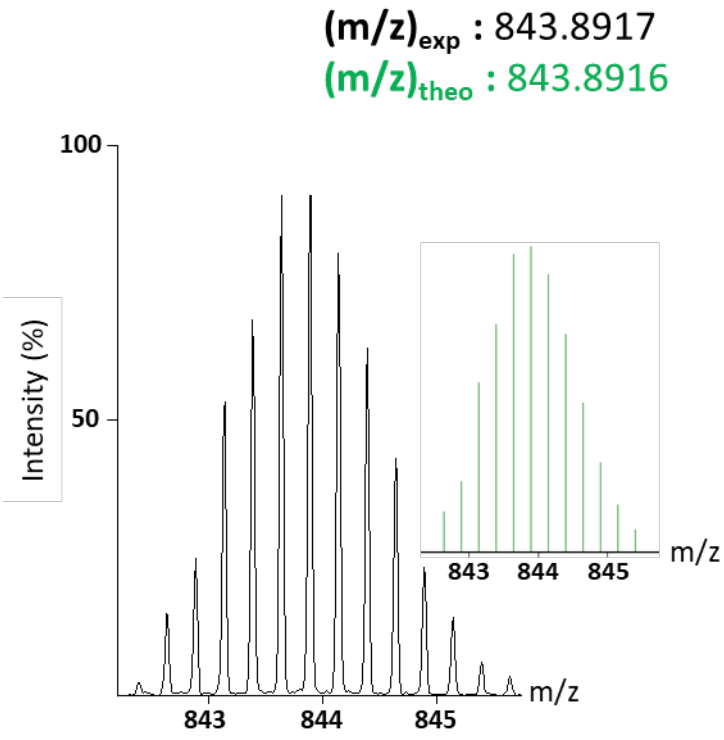

**Figure S3 Surface zeta-potential of 4@ and 3@**: Surface zeta-potential of (**A**) **4@** and (**B**) **3@** measured in 1.0 mM PBS buffer using a zeta-nanosizer.

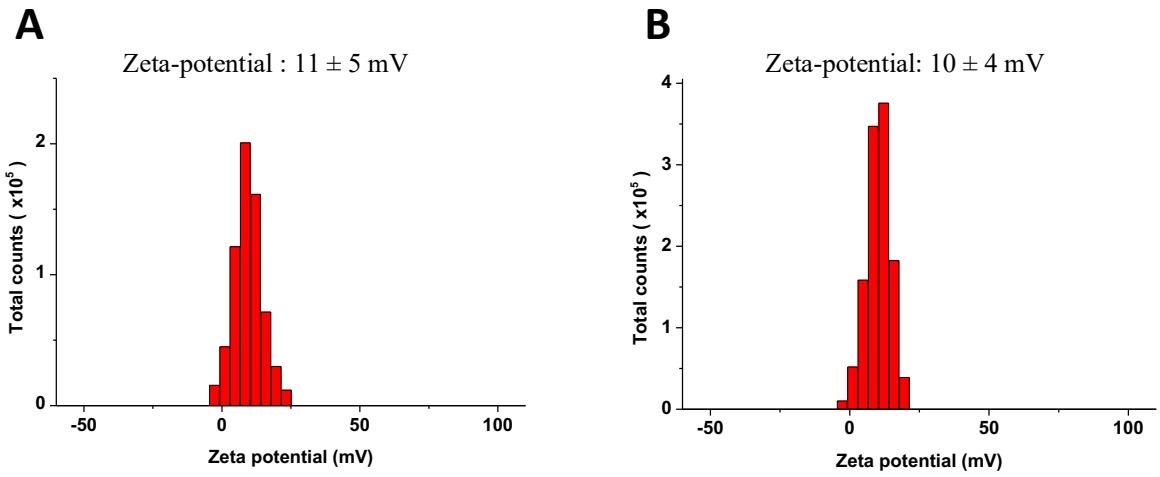

**Figure S4 Computer simulations of 3@ and 4@**: Zoomed snapshot of **3**@ (**A**) and **4**@ (**B**) as extracted from the equilibrated portion of the corresponding molecular dynamics (MD) trajectories. The Ga atoms are highlighted in red. Water molecules and counterions are omitted for the sake of clarity. Radial distribution function (RDF) of the hydrophobic tails (light green or light blue) and the Ga-bearing terminals (red) as a function of the distance from the center of mass ($r_{COM}$) for **3**@ (**C**) and **4**@ (**D**) calculated from the equilibrated portions of their MD trajectories.

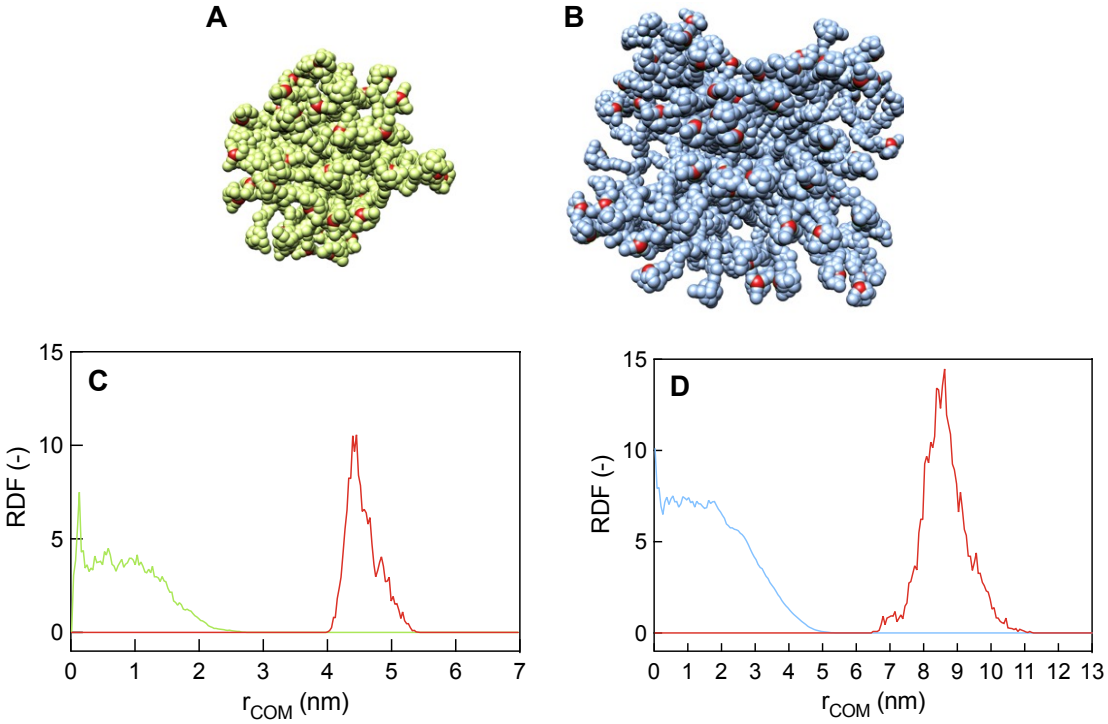

## Materials and methods

**AD-1** and **AD-2** were synthesized according to the established protocols.[1,2] NODA-GA($tBu$)$_3$ was purchased from CheMatech (Dijon, France). Other chemicals were purchased from Acros Organics, Sigma Aldrich or Alfa Aesar. Ethylenediamine was distilled before use. The other chemicals were used without further purification. Dialysis tubing was purchased from Sigma Aldrich (St. Quentin Fallavier, France). Analytical thin layer chromatography (TLC) was performed using silica gel 60 $F_{254}$ plates 0.2 mm thick with iodine as revelator. Chromatography was prepared on silica gel (Merck 200-300 mesh). IR spectra were recorded with an ALPHA FT-IR spectrometer (Bruker, France). $^{1}$H NMR spectra were recorded at 400 or 500 MHz and $^{13}$C NMR spectra recorded at 100 MHz on Bruker Avance III 400, or JEOL ECS 400 spectrometers. Chemical shifts (δ) are expressed in parts per million (ppm) with the residual peak of $CHCl_3$ at 7.26 ppm or $CH_3OH$ at 3.31 as internal reference. Radiolabeling analyses were performed on instant thin layer chromatography (iTLC) with a MiniGITA radiochromatography system (Elisia-Raytest, Angleur, Belgium).

## Nuclear Magnetic Resonance

Nuclear Magnetic Resonance (NMR) experiments were acquired at 300K using a Bruker Avance DRX 500 NMR spectrometer (Karlsruhe, Germany) operating at 500.13 MHz for $^{1}$H and 125.14 MHz for $^{13}$C Larmor frequency with a double resonance broadband fluorine observe (BBFO) 5 mm probe head. $^{13}$C-NMR experiments were recorded using one-pulse excitation pulse sequence (90° excitation pulse) with $^{1}$H decoupling during signal acquisition (performed with WALTZ-16); the relaxation delay has been set at 2 s. For each analyzed sample, depending on the compound concentration, 3k up to 5k free induction decays (FID) 64k complex data points were collected using a spectral width of 30000 Hz (240 ppm).[3]

## Mass Spectrometry

High resolution mass spectrometry experiments were performed with a Synapt G2 HDMS quadrupole/time-of-flight (Manchester, UK) equipped with an electrospray

source operating in positive mode. Samples were introduced at 10 µL/min flow rate (capillary voltage +2.8 kV, sampling cone voltage: varied between -80 V and +50 V) under a curtain gas ($N_2$) flow of 100 L/h heated at 35 °C. Accurate mass experiments were performed using reference ions from $CH_3COONa$ internal or external standard. The samples were dissolved and further diluted in methanol (Sigma-Aldrich, St-Louis - MO, USA) doped with acetic acid (1% v/v) prior to analysis. Data analyses were conducted using MassLynx 4.1 programs provided by Waters.

**Synthesis and characterization of the amphiphilic dendrimer 3**

The synthesis and characterization of **3** was carried out as described in our previous work.[4]

**Synthesis and characterization of AD-3**

To a mixture of **AD-2** (182 mg, 0.19 mmol) and CuI (19 mg, 0.10 mmol) in DMF (4.0 mL) under argon, was added a solution of **AD-1** (124 mg, 0.20 mmol) in DMF (3.0 mL). Then 1.8-diazabicyclo(5,4,0)undec-7-ene (DBU) (148 µL, 0.99 mmol) was added into the reaction mixture. The resulting solution was stirred at 60 °C for 3 h under argon until the reaction was completed as indicated by TLC. Then DMF was removed under reduced pressure, the obtained residue was suspended in 15 mL of 0.10 mM EDTA solution to remove the copper and extracted with $CH_2Cl_2$ (12 mL × 3). The combined organic layers were washed successively with saturated brine solution (15 mL × 2). The organic phase was dried with $MgSO_4$, filtrated and concentrated. The product was purified by column chromatography with $CH_2Cl_2$/MeOH/ammonia (v/v/v: 88/11.5/0.5) giving the corresponding **AD-3** as a yellow solid (171 mg, yield = 55%). $^1$H NMR (400 MHz, CDCl3): δ 7.84 (br s, 2H, -NH-), 7.69 (s, 1H, -CH- triazole), 7.19 (br s, 2H, -NH-), 6.91 (br s, 2H, -NH-), 4.52 (t, 2H, *J* = 4.6 Hz, -CH2-), 3.88 (t, 2H, *J* = 4.4 Hz, -CH2-), 3.83 (s, 2H, -CH2-), 3.66 (s, 12H, -OCH3), 3.56-3.51 (m, 4H, -CH2-), 3.46 (t, 2H, *J* = 4.8 Hz, -CH2-), 3.34-3.27 (m , 12H, -CH2-), 2.79-2.73 (m, 16H, -CH2-), 2.63-2.61 (m, 2H, - CH2-), 2.54 (t, 4H, *J* = 5.6 Hz, -CH2-), 2.45-2.41 (m, 12H, -CH2-), 2.35-2.331 (m, 4H, -CH2-), 2.16 (t, 4H, *J* = 7.6 Hz, -CH2-), 1.59 (s, 4H, -CH2-), 1.24 (s, 56H, -CH2-), 0.87

(t, 6H, *J* = 6.6 Hz, -CH3); $^{13}$C NMR (100 MHz, CDCl3): δ 174.2, 173.4, 173.0, 172.1, 143.8, 123.8, 70.5, 70.2, 69.4, 68.9, 52.9, 51.6, 50.6, 50.1, 49.2, 47.6, 40.1, 39.1, 37.1, 36.7, 34.0, 33.7, 32.7, 31.9, 29.7, 29.5, 29.4, 29.3, 25.8, 22.6, 14.1. HRMS-ESI(+): calculated isotopic maximum at *m/z* 782.0774 for $C_{81}H_{153}N_{13}O_{16}^{2+}$; found at *m/z* 782.0776 (+0.2 ppm).

**Synthesis and characterization of AD-4**

To a solution of **AD-3** (80 mg, 0.050 mmol) in methanol (5.0 mL) was added ethylenediamine (3.5 mL, 52.5 mmol). The reaction mixture was stirred for 72 h at 30 °C under argon. When the reaction was completed as indicated by IR analysis, the reaction solution was evaporated to remove the solvent, the resulting residue was purified by dialysis using dialysis tube of MWCO 2000 (Dialysis tubing from Sigma Aldrich. St. Quentin Fallavier, France) followed by lyophilization. After repeating 4 times the operation of dialysis and lyophilization, the product **AD-4** (81 mg, yield = 95%) was obtained as a white solid. $^{1}$H NMR (400 MHz, CDCl3/CD3OD = 3/1): δ 7.56 (s, 1H, -CH- triazole), 3.62 (t, 2H, J = 4.8 Hz, -CH2-), 3.53 (s, 2H, -CH2-), 3.32-3.24 (m, 6H, -CH2-), 3.07-2.94 (m, 26H, -CH2-), 2.51-2.39 (m , 20H, -CH2-), 2.28 (t, 4H, J = 6.4 Hz, -CH2-), 2.16-2.01 (m, 16H, -CH2-), 1.90 (t, 4H, J = 7.4 Hz, -CH2-), 1.31 (s, 4H, -CH2-), 0.98 (s, 56H, -CH2-), 0.60 (t, 6H, J = 6.2 Hz, -CH3); $^{13}$C NMR (100 MHz, $CDCl_3$/$CD_3OD$ = 3/1): δ 174.7, 173.4, 172.7, 142.7, 124.0, 69.9, 69.7, 68.8, 68.4, 52.1, 51.8, 49.6, 40.9, 40.3, 38.7, 38.4, 36.9, 35.9, 33.2, 32.9, 31.4, 29.2, 29.1, 28.9, 28.8, 25.4, 22.1, 13.4; HRMS-ESI(+): calculated isotopic maximum at *m/z* 838.1625 for $C_{85}H_{169}N_{21}O_{12}^{2+}$; found at *m/z* 838.1622 (+0.3 ppm).

**Synthesis and characterization of the amphiphilic dendrimer AD-NOTA**

To a solution of NODA-GA(*t*Bu)$_3$ (125 mg, 0.23 mmol) in anhydrous DMF (2.0 mL) were added PyBOP (119 mg, 0.23 mmol) and NMM (29 mg, 0.29 mmol). The mixture was stirred for 15 min and then a solution of **AD-4** (32 mg, 0.019 mmol) in anhydrous DMF (1.0 mL) and anhydrous DCM (2.0 mL) was added, and the resulting mixture was stirred at 30 °C for 3.0 days under argon. After 3 days, the reaction mixture was

evaporated under reduced pressure to remove the solvents, and the residue was dissolved in DCM (10 mL) and washed with water (5 mL × 2), saturated $NaHCO_3$ solution (5 mL × 2), and brine solution (5 mL × 2). The organic layers were collected and dried over anhydrous $Na_2SO_4$, and then the solvent was removed with a rotary evaporator at 30 °C. The obtained product was purifying by 3 rounds of precipitation in DCM/pentane. The purified dendrimer was dissolved in a TFA/$CH_2Cl_2$ mixture (3.0 mL, v/v = 1/1) and stirred at 30 °C for 24 h under argon. After evaporating the solvent, the crude residue was purified by dialysis (dialysis tubing, MWCO 2000 from Sigma Aldrich. St. Quentin Fallavier, France) and lyophilization. Repeating the operation cycles of dialysis (change dialysis water every hour for 8 h) and lyophilization for 4 times, yielded the corresponding **AD-NOTA** as a white fluffy solid (42 mg, yield = 71 %). $^{1}$H NMR (500 MHz, $CDCl_3$/$CD_3OD$): δ 7.72 (s, 1H), 4.26 (s, 2H), 3.87-3.50 (m, 30H), 3.50-2.46 (m, 112H), 2.41-1.99 (m, 16H), 1.89-1.77 (m, 10H), 1.26 (t, 4H), 1.02-0.87 (br, 56H), 0.62-0.51 (t, 6H); $^{13}$C NMR (126 MHz, $CDCl_3$/$CD_3OD$): δ175.2, 174.6, 174.0, 172.4, 171.4, 70.3, 70.2, 69.1, 64.7, 57.1, 52.5, 52.0, 51.4, 50.0, 49.6, 38.9, 38.8, 36.2, 32.6, 31.8, 29.5, 29.4, 29.3, 29.2, 25.7, 24.7, 22.5, 13.6. HRMS-ESI(-): calculated isotopic maximum at *m/z* 1033.6353 for $C_{145}H_{256}N_{33}O_{40}^{3-}$; found at *m/z* 1033.6357 (+0.4 ppm).

**Synthesis and characterization of the amphiphilic dendrimer 4**

The dendrimer **AD-NOTA** (5.1 mg, 1.6 µmol) was dissolved in 3.0 mL of $H_2O$. To this solution was added the solution of [$^{69}$Ga]$GaCl_3$ (1.3 mg, 7.3 µmol) in 1.0 mM HCl and the pH value was adjusted to 4.5 with addition of 0.2 M ammonium acetate. The mixture was incubated for 15 min at pH 4.5 at 25 °C. The obtained crude product was purified by dialysis for one day (dialysis tubing, MWCO 2000 from Sigma Aldrich. St. Quentin Fallavier, France), then lyophilized to give a white powder **4**. (5.0 mg, yield = 90%). ESI(+)-HRMS: calculated isotopic maximum at m/z 843.8916 for $C_{145}H_{251}Ga_4N_{33}O_{40}^{4+}$; found at m/z 843.8917 (+0.1 ppm).

**Dynamic light scattering (DLS)**

Dynamic light scattering (DLS) measurements were performed to determine the hydrodynamic diameter and zeta potential of the nanoparticles formed with **3** and **4**, respectively. The dendrimer was first dispersed in milliQ water at a concentration of 0.50 mg/mL, and sonicated 30 seconds at 60 Hz (Ultrasonic Cleaner Branson B-200), then the fresh solution was measured using a Malvern Zetasizer Nano ZS equipped with a standard 633 nm laser at 25 °C. The experiments were done in triplicates.

**Transmission Electron Microscopy (TEM)**

Transmission electron microscopy (TEM) was performed using JEOL 2100F analytical electron microscope (Tokyo, Japan) to characterize the size and morphology of the NPs at an accelerating voltage of 300 kV. The dendrimer was dispersed in milliQ water at a concentration of 1.0 mg/mL, and sonicated for 30 seconds, then diluted to 1.6 µg/mL, followed by depositing an aliquot (4.0 µL) onto a carbon-coated copper grid and dried for 15 minutes at 37 °C. The grid was then stained with 3.0 µL uranyl acetate (2.0 % in aqueous solution) for 4 seconds, and the excess uranyl acetate was removed by filter paper before measurements. The nanoparticle diameter was measured using ImageJ software, analyzing over 50 particles. The standard deviation was calculated to assess variability within the dataset.

**Critical micelle concentration (CMC)**

CMC was determined using Nile Red as a fluorescence probe. Dendrimer **4** solution at different concentrations varied from 0.10 to 40 µM were prepared and the final Nile Red concentration was 3.0 µM in water. The solutions were vortexed for 10 min and kept for 2 h at room temperature to promote the micelle formation prior to fluorescence measurement. Fluorescence spectra were recorded at the emission wavelength of 635 nm on F-4500 fluorescence spectrophotometer at room temperature. Excitation wavelength is 550 nm. The normalized fluorescence intensity was analyzed as a function of micelle concentration.

**Isothermal titration calorimetry (ITC)**

Isothermal titration calorimetry (ITC) experiments were performed with a MicroCal PEAQ-ITC calorimeter (Malvern, UK) at 298 K. The cell volume was 208 µL. The micellization experiments were conducted by step-by-step injections of a constant volume of concentrated **3@** or **4@** solution into the calorimetric cell containing ultra-pure water. Specifically, a constant 2 µL portion of the amphiphilic dendrimer solution, at a concentration of 850 µM for **3** and of 350 µM for **4**, was injected 18 times into the reaction cell at 150 s intervals. Upon filling cell and syringe, stirring was turned on and the system was allowed to thermally equilibrate for 30 minutes. The integrated ITC data were fitted to a sigmoidal function to yield the free enthalpy of micellization, $\Delta H_{mic}$, as the difference between the final and the initial values of the integrated heat of the titration curve. The CMC is defined as the midpoint of the same curve. The free energy of micellization ($\Delta G_{mic}$) is given by the expression $\Delta G_{mic} = RT \ln CMC'$, where R is the gas constant ($1.987\times10^{-3}$ kcal/mol K), T is the absolute temperature, and CMC' is the critical micellization concentration expressed in molar fraction. The change in entropy associated with the micellization ($T\Delta S_{mic}$) is calculated from the second law of thermodynamics by using the Gibbs–Helmholtz equation $T\Delta S_{mic} = \Delta H_{mic} - \Delta G_{mic}$. Finally, the aggregation number ($N_{agg}$) was estimated from the same data set using a protocol based on the two-state reaction model and the principle of mass conservation.[5,6]

**Computer simulations**

All simulations were carried out using AMBER 23[7] on a CPU/GPU hybrid cluster and the pre-exascale Tier-0 EuroHPC Leonardo supercomputer (CINECA, Bologna, Italy). Graphics and analysis were performed using the UCSF Chimera software[8] and the GraphPad Prism (v. 9) (GraphPad Software, www.graphpad.com). The monomers **3** and **4** were parametrized following a well-established procedure[9]. Atom types were assigned via Antechamber of AmberTools with Gaff2 atom types[10] and the Visual Force Field Derivation Toolkit (VFFDT)[11]. Based on the ITC experiments, fifteen (15) monomers of **3** and twenty (20) monomers of **4** were randomly placed in a cubic box filled with TIP3 waters[12] extending at least 20 Å from each solute molecule. System neutralization was achieved by adding the appropriate number of chloride

counterions. The prepared systems underwent a combination of steepest descent and conjugate gradient minimization of the potential energy, followed by gradual heating to 298 K through 500 ps of atomistic molecular dynamics (MD) simulations in the canonical (NVT) ensemble under periodic boundary conditions. The SHAKE algorithm[13] was applied to all covalent bonds involving hydrogen atoms. An integration time step of 2.0 fs was used, along with the Langevin thermostat for temperature regulation[14]. The final heating step was followed by 50 ns of MD equilibration in the isochoric/isothermal (NPT) ensemble. Pressure control was maintained using a Berendsen barostat[15]. The Particle Mesh Ewald (PME)[16] method was used to treat long-range electrostatic interactions under periodic conditions with a direct space cut-off of 10 Å. Finally, the NPT MD production run was performed for additional 500 ns.

**Radiolabeling of [$^{68}$Ga]-4 and [$^{68}$Ga]-3**

Radiosynthesis of dendrimers **3** and **4** was carried out as previously validated.[4] Eighty microliters of 1.0 mol.L$^{-1}$ ammonium acetate buffer (pH 7.4) were added to a 50 µL (1 µg/µL) of dendrimer **4** solution. 500 µL of [$^{68}$Ga]$GaCl_3$ (85.3±17.9 MBq/500 µL) (n = 3) were eluted from a commercial TiO2-based [$^{68}$Ge]Ge/[$^{68}$Ga]Ga generator (Galliapharm, Eckert & Ziegler Berlin, Germany) using 0.1 mol.L$^{-1}$ HCl and added to the reactor. Final pH measure for the radiotracer solution containing dendrimer **4** was 5.0. Reaction was carried at room temperature (25 °C) for 10 minutes. Radiochemical purity (RCP) was evaluated by radio-thin layer chromatography on glass microfiber chromatography paper impregnated with silica gel (iTLC plate) with mobile phase in 0.1 mol.L$^{-1}$ sodium citrate buffer (pH = 5) at the end of radiosynthesis.

**Radiolabeling stability of [$^{68}$Ga]-4**

The radiolabeling stability of **[$^{68}$Ga]Ga-4** (n = 3) was assessed after incubation of 100 µL of the radiotracer in 400 µL of physiological saline (NaCl 0,9%) or 400 µL of human serum at room temperature, and at 37 °C. The RCP was checked at 60, 120, 180, and 240 minutes after radiosynthesis by radio-TLC.

**Animals**

All procedures involving animals were approved by the Institution's Animal Care and Use Committee (CE71, Aix-Marseille Université, project #14191), conducted according to the 2010/63/EU European Union Directive and the ARRIVE guidelines 2.0. Mice were housed in enriched cages and placed in a temperature- and hygrometry-controlled room with daily monitoring, fed with water, and commercial diet *ad libitum*.

**PET/CT and gamma-counting biodistribution**

Fifteen-week-old male CD-1/Swiss mice (n = 4, Janvier Labs, Le Genest, France) were injected in the lateral caudal vein with [$^{68}$Ga]Ga-3 (3.52±1.0 MBq/100µL) or [$^{68}$Ga]Ga-4 (3.86±0.85 MBq/100 µL). Dynamic PET/CT images were acquired continuously for 120 min post-injection on a NanoScan PET/CT camera (Mediso, Budapest, Hungary) under 3% sevoflurane in medical air anesthesia with the following PET parameters: number of interactions 4, coincidence 1-3, field of view (FOV): 9.82 cm; CT parameters were fixed at 35kV voltage, 300 ms exposure, acquired at semi-circular method on the same FOV as for PET. CT attenuation-corrected reconstruction was performed using Nucline software (v. 3.04, Mediso, Budapest, Hungary) on the following time frames: 0–5 min, 6–10 min, 11–15 min, 16–20 min, 21–25 min, 26–30 min, 31–45 min, 46–60 min, 61–75 min, 76–90 min, 91–105 min, and 106–120 minutes. PET signals in organs were quantified by manually drawn volumes of interest (VOI) on the PET/CT images using the VivoQuant software (v. 4.0, InVicro, Boston, USA). Quantification results were presented as mean ± SD percentage of decay-corrected injected dose per centimeter cube of tissue (%ID/cm$^3$). At the end of the PET/CT acquisition, mice were euthanatized, and the main organs (liver, heart, kidneys, lungs, brain, spleen, pancreas, muscle, and bones) were collected, washed in physiological saline, weighted, and gamma counted (Hidex AMG, Hidex Oy, Turku, Finland). Results were decay-corrected and expressed as percentage of injected dose corrected per gram (%ID/g). Statistical analyses were performed using Prism (v.9, GraphPad, San Diego,

USA), $P \leq 0.05$ indicating statistical significance. Signal and accumulation in each organ were compared using one-way ANOVA test.

Fifteen-week-old male CD-1/Swiss mice (n = 4, Janvier Labs) were injected in the lateral caudal vein with [$^{68}$Ga]Ga-3 (3.87±0.2 MBq/100µL) or [$^{68}$Ga]Ga-4 (3.9±0.9 MBq/100 µL), and maintained under 3% sevoflurane in medical air anesthesia for 120 minutes. 20 µL of blood were collected at 5, 15, 30, 45, 90, and 120 minutes post-injection and gamma-counted. After decay and blood volume corrections, results were expressed as percentage of injected dose (%ID).

**Statistics**

Statistical analyses were conducted using Prism (v.10.0.2, GraphPad, San Diego, USA), with P≤0.05 considered statistically significant. The quantified activities of each radiotracer in the organs were compared using a two-way ANOVA test followed by a Šídák's multiple comparisons test. Blood quantifications were analyzed using non-linear, two-phase decay least-squares regression to calculate the plasmatic half-life.

**Reference**


1. Yu,. T. *et al.* An Amphiphilic Dendrimer for Effective Delivery of Small Interfering RNA and Gene Silencing In Vitro and In Vivo. *Angew. Chem. Int. Ed.* **51**,. 8478–8484 (2012).
2. Liu, X. *et al.* Adaptive amphiphilic dendrimer based nanoassemblies as robust and versatile siRNA delivery systems. *Angew Chem Int Ed Engl* **53**, 11822–11827 (2014).
3. Braun, S. 150 and more basic NMR experiments : a practical course /. (1998).
4. Garrigue, P. *et al.* Self-assembling supramolecular dendrimer nanosystem for PET imaging of tumors. *Proc Natl Acad Sci USA* **115**, 11454–11459 (2018).

5. Olesen, N. E., Westh, P. & Holm, R. Determination of thermodynamic potentials and the aggregation number for micelles with the mass-action model by isothermal titration calorimetry: A case study on bile salts. *Journal of Colloid and Interface Science* **453**, 79–89 (2015).

6. Laurini, E. *et al.* ITC for Characterization of Self-Assembly Process of Cationic Dendrons for siRNA Delivery. in *Design and Delivery of SiRNA Therapeutics* (eds. Ditzel, H. J., Tuttolomondo, M. & Kauppinen, S.) 245–266 (Springer US, 2021). doi:10.1007/978-1-0716-1298-9_15.

7. D.A. Case, H.M. Aktulga, K. Belfon, I.Y. Ben-Shalom, J.T. Berryman, S.R. Brozell, D.S. Cerutti, T.E. Cheatham, III, G.A. Cisneros, V.W.D. Cruzeiro, T.A. Darden, N. Forouzesh, G. Giambaşu, T. Giese, M.K. Gilson, H. Gohlke, A.W. Goetz, J. Harris, S. Izadi, S.A. Izmailov, K. Kasavajhala, M.C. Kaymak, E. King, A. Kovalenko, T. Kurtzman, T.S. Lee, P. Li, C. Lin, J. Liu, T. Luchko, R. Luo, M. Machado, V. Man, M. Manathunga, K.M. Merz, Y. Miao, O. Mikhailovskii, G. Monard, H. Nguyen, K.A. O'Hearn, A. Onufriev, F. Pan, S. Pantano, R. Qi, A. Rahnamoun, D.R. Roe, A. Roitberg, C. Sagui, S. Schott-Verdugo, A. Shajan, J. Shen, C.L. Simmerling, N.R. Skrynnikov, J. Smith, J. Swails, R.C. Walker, J. Wang, J. Wang, H. Wei, X. Wu, Y. Wu, Y. Xiong, Y. Xue, D.M. York, S. Zhao, Q. Zhu, and P.A. Kollman (2023), Amber 2023, University of California, San Francisco.

8. Pettersen EF, Goddard TD, Huang CC, Couch GS, Greenblatt DM, Meng EC, Ferrin TE. UCSF Chimera--a visualization system for exploratory research and analysis. J Comput Chem. 2004 Oct;25(13):1605-12.

9. Garrigue P, Tang J, Ding L, Bouhlel A, Tintaru A, Laurini E, Huang Y, Lyu Z, Zhang M, Fernandez S, Balasse L, Lan W, Mas E, Marson D, Weng Y, Liu X, Giorgio S, Iovanna J, Pricl S, Guillet B, Peng L. Self-assembling supramolecular dendrimer nanosystem for PET imaging of tumors. Proc Natl Acad Sci U S A. 2018 Nov 6;115(45):11454-11459.

10 Träg, J., Zahn, D. Improved GAFF2 parameters for fluorinated alkanes and mixed hydro- and fluorocarbons. J Mol Model 25, 39 (2019).

11. Zheng S, Tang Q, He J, Du S, Xu S, Wang C, Xu Y, Lin F. VFFDT: a new software for preparing AMBER force field parameters for metal-containing molecular systems. Journal of chemical information and modeling. 2016;56:811-818.

12 W. L. Jorgensen, J. Chandrasekhar, J. D. Madura, R. W. Impey and M. L. Klein, J. Comparison of simple potential functions for simulating liquid water. Chem. Phys., 1983, 79, 926.

13 J.-P. Ryckaert, G. Ciccotti and H. J. C. Berendsen, Numerical integration of the cartesian equations of motion of a system with constraints: molecular dynamics of n-alkanes. J. Comput. Phys., 1977, 23, 327.

14 X. Wu and B. R. Brooks, Self-guided Langevin dynamics simulation method. Chem. Phys. Lett., 2003, 381, 512.

15 H. J. C. Berendsen, J. P. M. Postma, W. F. van Gunsteren, A. DiNola, and J. R. Haak, Molecular dynamics with coupling to an external bath, J Chem Physi 81, 3684-3690 (1984).

16 T. Darden, D. York and L. Pedersen, Particle mesh Ewald: An N·log(N) method for Ewald sums in large systems. J. Comput. Phys., 1993, 98, 10089.